Magnetoelectric Effect in Bi5Ti3FeO15 Ceramics Obtained by Molten Salts Synthesis

L. Fuentes, M. García, D. Bueno, M. E. Fuentes & A. Muñoz

The synthesis and magnetoelectric characterization of multiferroic Bi5Ti3FeO15 is presented. Samples were obtained by the molten-salts method. Structural analysis was per-formed by means of electron microscopy and x-ray diffraction. The increase of plate-like crystallites' dimensions with increasing reaction temperature is characterized. Magnetoelectric parameters are measured under a pulsed magnetic field of 2·104 Oe amplitude. Textured polycrystalline ceramics are property cut and electrically polarized. Longitudinal and transversal magnetoelectric voltages are sensed, from liquid-nitrogen to room temperatures. Only low-temperature transverse magnetoelectric effect is observed as significant.

Keywords Magnetoelectricity; multiferroics; Aurivillius phases; molten salt synthesis

Introduction

The search for single-phased magnetoelectric (ME) multiferroics is an important challenge of present day's active-materials science [1]. A limited number of perovskites [2, 3] and other selected phases [4] have been reported to exhibit the mentioned property. Some so-called Aurivillius phases are included in the list of privileged compounds [5]. A couple of difficulties regarding trustable ME characterization of Aurivillius ceramics may be pointed out. a) Even though axial nature of ME tensor should lead to careful investigation of longitudinal versus

transverse response in a ME sample, references to this consideration are scarce [6]. b) Reported experimental values for ME coefficients of specific phases show significant dispersion in the literature. Observe, for example, the discrepancy of one order of magnitude between the figures reported in references [7] and [8] for the Aurivillius compound Bi5Ti3FeO15 (BFT).

The aim of the present article is to divulge a couple of modest contributions to the ME characterization of the Aurivillius BFT phase: a) A study of the molten salt synthesis (MSS) of this phase. b) A texture-oriented measurement of ME coefficients under pulsed magnetic fields.

Materials and Methods

Stoichiometric quantities of (≥99.9%, Fisher/Baker) metallic oxides were homogenized, with an equimolar mixture of NaCl and KCl, in a zirconia mortar. Reagent masses were calculated according to the equation:

$$3TiO_2 + 1/2Fe_2O_3 + 5/2Bi_2O_3 \rightarrow Bi_5Ti_3FeO_{15}.$$

0 g masses (2 g oxides, 8 g chlorides) were deposited in covered alumina crucibles and put to react for 6 h at T = 700, 750, . . . , 950 C. Heating and cooling slopes were of 5 C/min. Before entering the maximum temperature range, the chlorides' mixture was fused at 675 C. After reaction, solid chlorides particles were washed out and Aurivillius crystals were dried at 110 C for 8 h. Solid polycrystalsceramics were obtained by sintering: Aurivillius powder was homogenized in polyvinyl alcohol, compacted under uniaxial pressure of 7000 kg/cm2 and heated gradually to 200, 500 and 1000 C. During sintering, a Bi-rich atmosphere in the vicinity of the sample was maintained.

Identification and structural characterization was performed by a combination of scanning electron microscopy (SEM-Jeol JSM 5800 LV) and x ray diffraction (XRD-Philips X'Pert MPD). XRD patterns were interpreted by application of the Rietveld Method [9]. Longitudinal and transverse ME coefficients were measured at CIMAV pulsed-field magnetoelectrometer, according to the methodology described by Ohtani and Khon [10].

Results on Synthesis

Figure 1 shows the XRD pattern of a sample synthesized at 850 C. Unique revealed phase is Bi5Ti3FeO15. Figure 2 represents the unit cell, as previously reported [11]. Space group is F2 mm and lattice parameters are (˚A): a = 5.4759(2), b = 5.4420(2), c = 41.157(1).

EM micrographs in Figs. 3 and 4 are representative of crystallite size and shape dependence on reaction temperature. Crystals are plate-shaped and their dimensions increase with increasing reaction temperature. Crystallites' large surfaces are parallel to bismuth oxide layers in Aurivillius phases.

Diffraction peaks in Fig. 1 exhibit small-crystallite-size broadening. Careful examination reveals a somewhat larger broadening for the (0, 0, l) peaks as compared with the (h,0,0)/(0, k, 0). Detected anisotropic broadening is caused by the plate-like shape of BFT crystals. Available Rietveld software [9] permits an approximation to crystal size and shape from pattern simulation. Figure 5 shows (0, 0, 10) peak broadenings for different reaction temperatures and Fig. 6 represents the XRD results for crystallite thickness and lateral dimensions as a function of temperature.

For all temperatures, broadening of (0, 0, l) diffraction peaks gives valuable information on crystallites' thickness. (h,0,0)/(0, k,0)peaks' broadening leads to an estimate of the lateral dimensions of crystallites. This kind of measurement reveals itself useful for T ≤ 800 C. For example, at T = 800 C, peak broadening gives th00 ≈ 860 ˚A = 86 nm, compatible with the TEM micrograph shown in Fig. 3. For T ≥ 850 C, diffraction (h,0, 0)/(0, k,0)peaks are too sharp to give crystallite size quantitatively. The XRD output is simply that crystallites are "large," comparable (at least) with a μm.

Magnetoelectric Performance

Electric spontaneous polarization in Aurivillius phases points essentially parallel to the surface of plate-crystals. Equation (1) and Fig. 7 characterize the appearance of a transverse

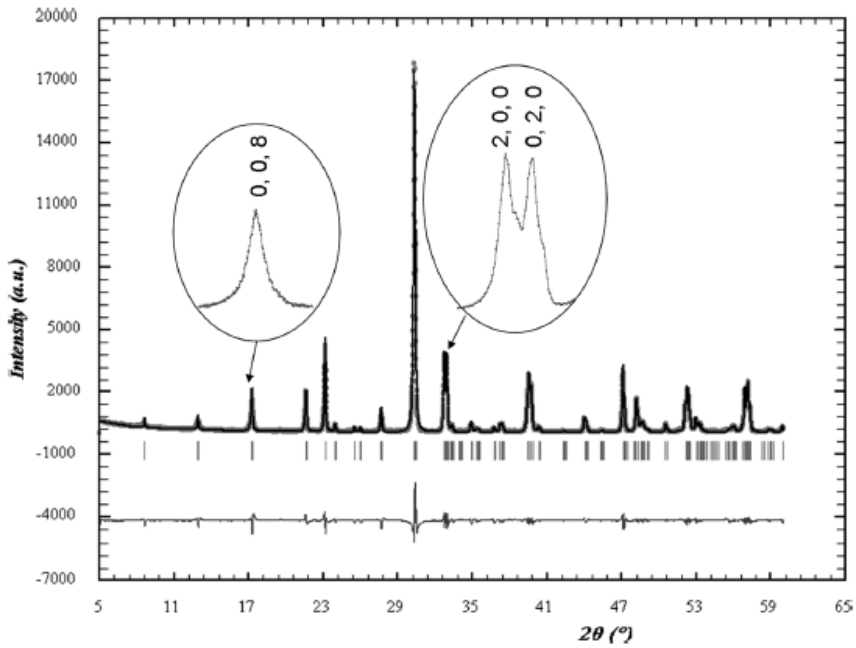

Figure 1. X-ray diffraction pattern of $Bi_5Ti_3FeO_{15}$. Reaction temperature = 850 C. (See Color Plate IX)

ME field (EME), generated by a particular magnetic excitation (H), in accordance with the ME tensor (α) that corresponds to point group 2 mm.

$$E_{ME} = \alpha \cdot H = \begin{bmatrix} 0 & 0 & 0 \\ 0 & 0 & \alpha_{23} \\ 0 & \alpha_{32} & 0 \end{bmatrix} \cdot \begin{bmatrix} 0 \\ H_2 \\ 0 \end{bmatrix} = \begin{bmatrix} 0 \\ 0 \\ \alpha_{32} H_2 \end{bmatrix}$$

Figure 8 describes the cutting and polarization of a textured polycrystal ceramic and equation (2) represents the average ME tensor <α> corresponding to the considered poarized configuration [12].

Uniaxial pressing generates a fiber texture with strong preference for crystal (0, 0, 1) plane normals to orient themselves parallel to fiber axis z. External electric field generates a macroscopic polarization along x.

$$\langle \alpha \rangle = \frac{2\alpha}{\pi}$$

Figure 9 is a plot of the longitudinal magnetoelectric surfaces α(h) associated to a BTF single crystal (outer surface) and to the texture of Fig. 8 (inner surface). Dark surfaces represent positive values of α(h) and light ones are negative. The following are some interesting features of the plot. a) Longitudinal response is null along the x, y and z axes. b) The xy and xz planes are ordinary-symmetry planes. Due to the axial nature of the ME tensor, the longitudinal ME surface changes sign under reflection on these planes.

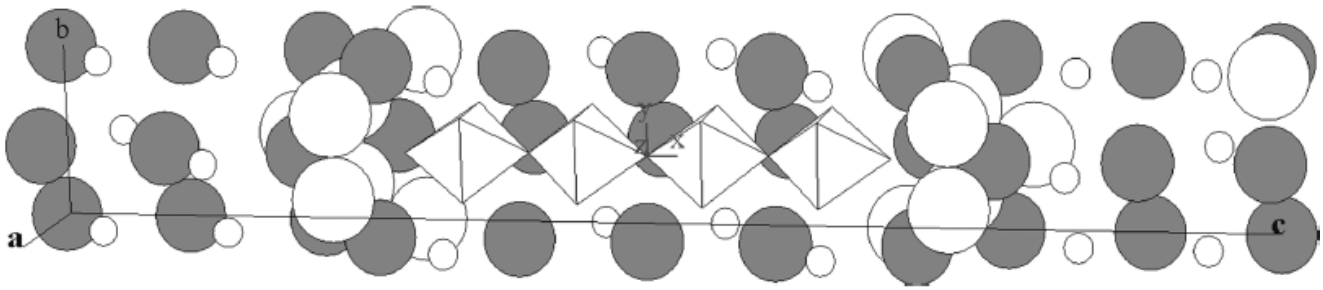

Figure 2. The crystal structure of $Bi_5Ti_3FeO_{15}$. Spheres: large white → O; small white → Ti; large gray → Bi. O atoms at the corners of Ti-coordination octahedra omitted. (See Color Plate X)

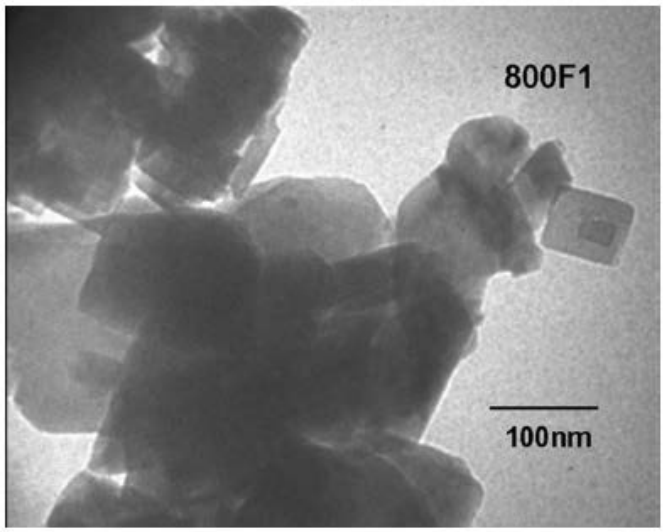

Figure 3. Transmission electron micrograph of $Bi_5Ti_3FeO_{15}$. Reaction temperature = 800

Finally, Fig. 10 is a plot of the magnetoelectric coefficient α32, measured on a poly-crystal sample of BFT. The conditions of the experiment are the following. Sample texture as described in Fig. 7, measurement under pulsed magnetic field (Hmax = 2·104 Oe), temperature = 150 K. The initial magnetoelectric coefficient is α32(H = 0) = 0.3 mV/cm·Oe. Longitudinal αii, same as all room-temperature coefficients, are null.

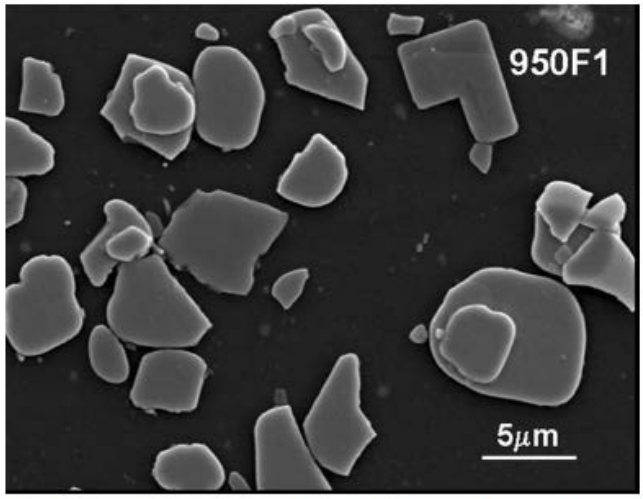

Figure 4. Scanning electron micrograph of $Bi_5Ti_3FeO_{15}$. Reaction temperature = 950 C.

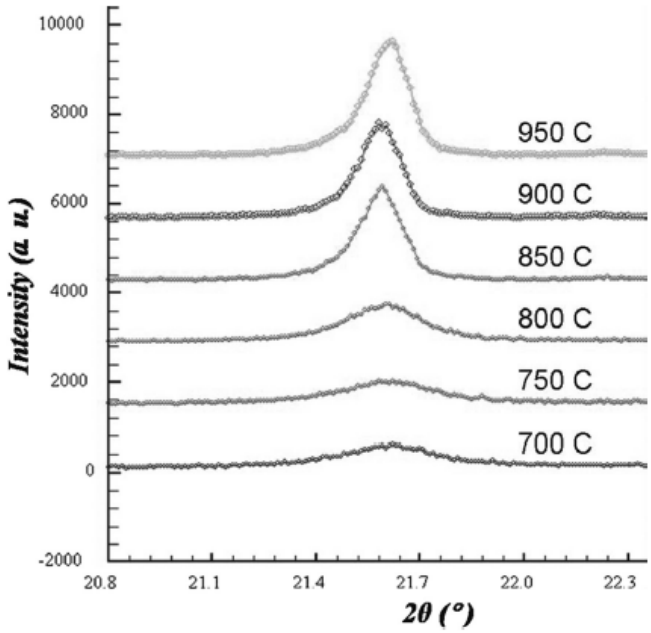

Figure 5. Broadening of XRD (0, 0, 10) peak as dependent of reaction temperature. (See Color Plate XI)

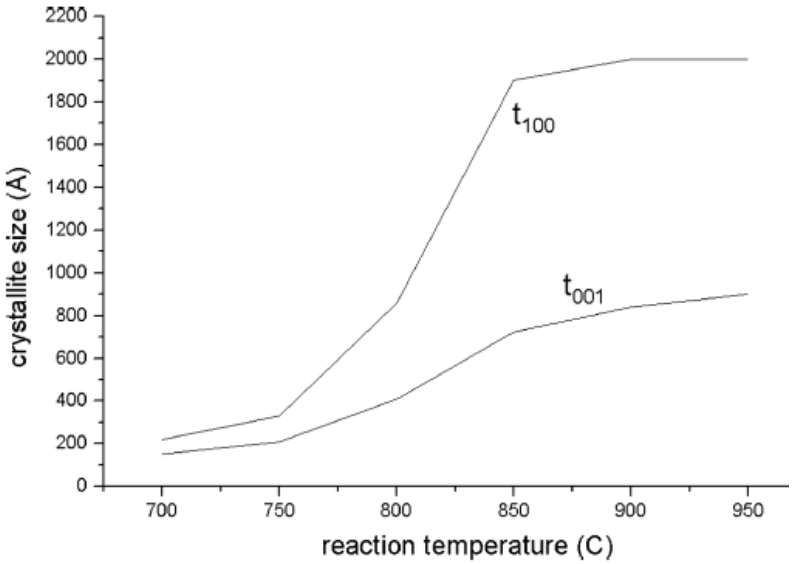

Figure 6. BFT crystal size and shape as function of reaction temperature.

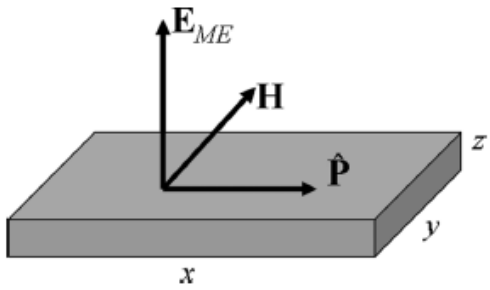

Figure 7. Electric polarization (P), magnetic field (H) and magnetoelectric field (E_{ME}) in a BFT plate-like crystallite. The relationship among the considered vectors may be expressed as a cross product: $E_{ME} = \alpha_{23} \hat{P} \times H$, with $\hat{P}$ denoting a unit vector in the direction of polarization.

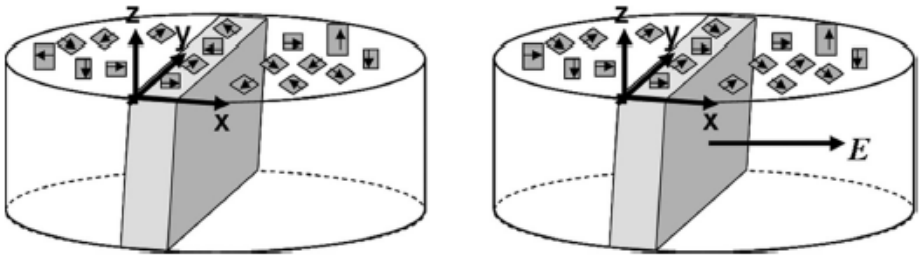

Figure 8. Cutting and polarization of a BFT textured ceramic.

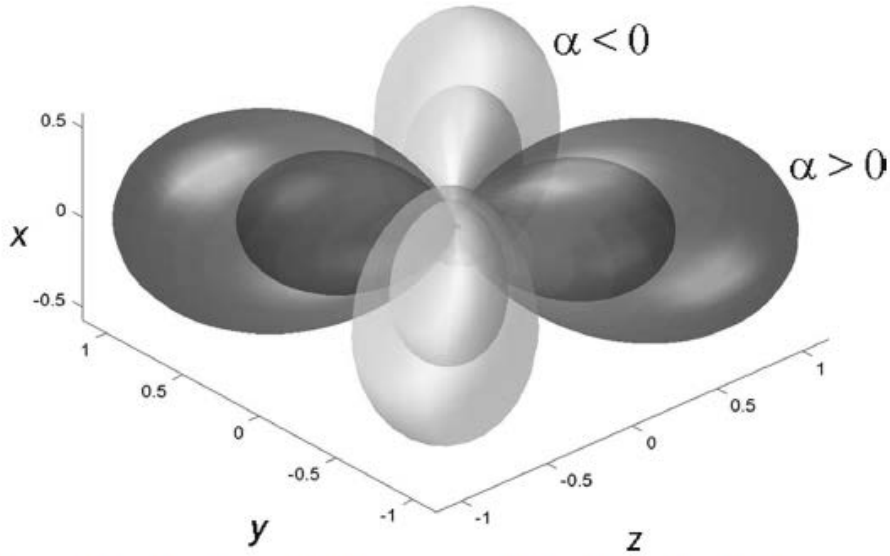

Figure 9. Longitudinal magnetoelectric surfaces $\alpha(h)$ for a BTF single crystal (outer surface) and for a textured and polarized polycrystal ceramic. (See Color Plate XII)

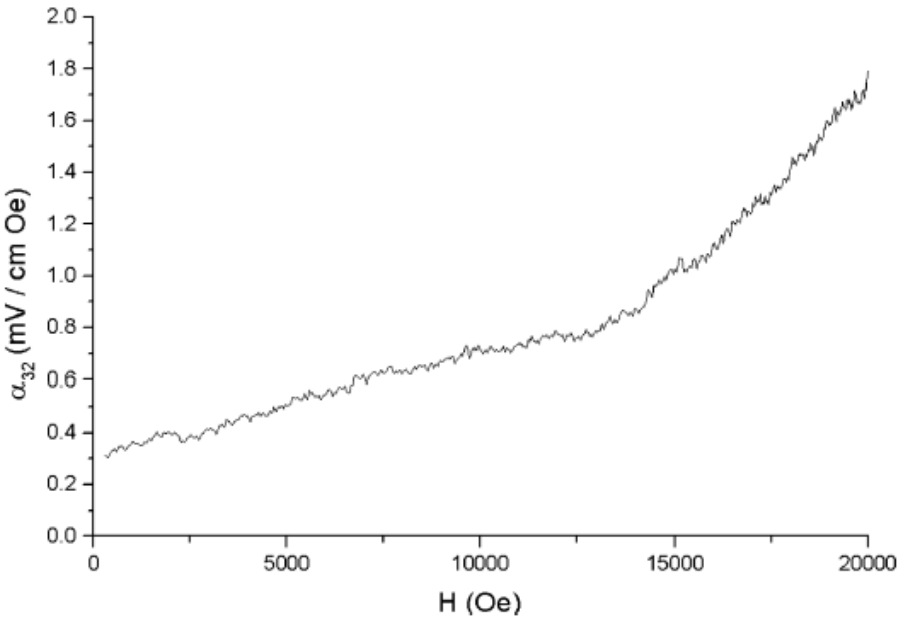

Figure 10. Transverse magnetoelectric coeffcicient α_{32} for the investigated BFT ceramic.

Acknowledgments

Portions of this research were carried out at the Stanford Synchrotron Radiation Laboratory, a national user facility operated by Stanford University on behalf of the U.S. Department of Energy, Office of Basic Energy Sciences. Support from CONACYT-Mexico (Project CIAM 42361: Multiferroic Materials) and from Program CYTED (Sub-Program VIII, Project VIII.13: Electroceramic Materials) is gratefully acknowledged.

References

1. N. A. Hill, Why are there so few magnetic ferroelectrics? J. Phys. Chem. B 104, 6694–6709 (2000).

2. J. Wang, J. B. Neaton, H. Zheng, et al., Epitaxial BiFeO3 multiferroic thin film heterostructures. Science 299, 1719–1722 (2003).

3. B. B. Van Aken, T. T. M. Palstra, A. Filippetti, and N. A. Spaldin, The origin of ferroelectricity in magnetoelectric YMnO3. Nature Materials 3, 164–170 (2004).

4. M.-H. Tsai, Y.-H. Tang, and S. K. Dey, Coexistence of ferroelectricity and ferromagnetism in 1.4 nm SrBi2Ta2O11 film. J. Phys. Condens. Matter 15, 7901–7915 (2003).

5. A. Srinivas, D.-W. Kim, and S. V. Suryanarayana, Study of magnetic and magnetoelectric mea-surements in bismuth iron titanate ceramic-Bi8Fe4Ti3O24. Mater. Res. Bull. 39(1), 55–61 (2004).

6. G. Srinivasan, E. T. Rasmussen, and R. Hayes, Magnetoelectric effects in ferrite-lead zirconate titanate layered composites: The influence of zinc

substitution in ferrites. Physical Review B 67, 014418 (2003).

7. A. Srinivas, S. V. Suryanarayana, G. S. Kumar, and M. M. Kumar, Magnetoelectric measurements on Bi5FeTi3O15 and Bi6Fe2Ti3O18. J. Phys. Condens. Matter 11, 3335–3340 (1999).

8. M. M. Kumar, A. Srinivas, S. V. Suryanarayana, G. S. Kumar, and T. Bhimasankaram, An experimental setup for dynamic measurement of magnetoelectric effect. Bulletin of Materials Science 21, 251–255 (1998).

9. http://ccp14.minerals.csiro.au/ccp/ccp14/ftp-mirror/fullprof/pub/divers/fullprof.2k/Windows/

10. J. Ohtani and K. Kohn, An apparatus for measuring magnetoelectric susceptibilities under pulsed high magnetic field. Rikogaku Kenkyusho Hokoku, Waseda Daigaku 102, 106–109 (1982).

11. M. Garcia-Guaderrama, L. Fuentes, M. E. Montero-Cabrera, A. Marquez-Lucero, and M. E. Villafuerte-Castrejon, Molten salt synthesis and crystal structure of Bi5Ti3FeO15. Integrated Fer-roelectrics 71, 233–239 (2005).

12. L. Fuentes, A. Rodriguez, G. Aquino de los Rios, and A. Mu˜noz-Romero, Modeling the influence of texture on the properties of electroceramics. Integrated Ferroelectrics 71, 289–301 (2005).